
Imaging DNA Synthesis In Vivo with ^{18}F -FMAU and PET

Haihao Sun, MD, PhD^{1,2}; Thomas J. Mangner PhD^{2,3}; Jerry M. Collins, PhD⁴; Otto Muzik, PhD^{2,5}; Kirk Douglas, MS^{1,2}; and Anthony F. Shields, MD, PhD^{1,2}

¹Department of Medicine, Wayne State University, Detroit, Michigan; ²Karmanos Cancer Institute, Wayne State University, Detroit, Michigan; ³Department of Radiology, Wayne State University, Detroit, Michigan; ⁴Food and Drug Administration, Rockville, Maryland; and ⁵Department of Pediatrics, Wayne State University, Detroit, Michigan

We imaged DNA synthesis in vivo with PET and ^{18}F -1-(2'-deoxy-2'-fluoro- β -D-arabinofuranosyl)thymine (FMAU), which is phosphorylated by thymidine kinases and incorporated into DNA. **Methods:** We produced ^{18}F -FMAU and injected the tracer into 5 normal dogs and studied them by imaging or biodistribution for up to 2.5 h. The pharmacokinetics of FMAU in blood and urine were determined using high-performance liquid chromatography analysis. At the end of each study, selected tissues were removed to measure the total activity retained in these tissues. In addition, the selected tissues were extracted by acid precipitation, by which the macromolecules can be precipitated to determine the radioactivity of ^{18}F -FMAU incorporated into DNA. **Results:** Imaging and tissue analysis showed increased activity in the lymph nodes, stomach, small intestine, and bone marrow, with mean standardized uptake values of 1.4, 1.6, 2.3, and 3.9, respectively, because of varying degrees of increased cell proliferation. In contrast, ^{18}F -FMAU was distributed with tissue-to-muscle ratios of approximately 1.0 in nonproliferative organs such as lung, liver, and kidneys. Analysis of the tissue extracts using acid precipitation demonstrated that 88% of activity in marrow and 65% of activity in small intestine was acid precipitated. However, more than 90% of activity in the nonproliferating tissues such as heart and lungs was in the supernatant. Increased activity was seen in the heart because of a high level of thymidine kinase 2 and in the gallbladder because of excretion. Analysis of blood and urine demonstrated that more than 95% of activity was present as intact ^{18}F -FMAU at the end of the studies. **Conclusion:** The results showed that ^{18}F -FMAU was selectively retained in DNA of the proliferating tissues and was resistant to degradation. These features indicate that ^{18}F -FMAU might be an alternative to ^{11}C -thymidine for imaging DNA synthesis in normal tissues and tumors.

Key Words: FMAU; PET; proliferation

J Nucl Med 2005; 46:292-296

PET can produce images of tumor physiology and thus has found increasing applications in oncology. On the basis of the tracer used, one can selectively measure several

metabolic pathways in vivo. This approach offers the opportunity to measure rapid metabolic changes in tumors after treatment (1-4). Increasing evidence indicates that PET is a sensitive approach to tumor detection and to evaluation of treatment response and that it complements anatomy-based techniques, which include physical examination, radiography, ultrasound, CT, and MRI.

^{18}F -FDG is currently the most commonly used agent for imaging tumors with PET. Although it has been used to stage and diagnose cancer and its uptake often declines after successful treatment (4), ^{18}F -FDG is not a highly selective tracer for tumor detection since glucose is used by many cell types. For instance, macrophages, which invade tumors and are also found in inflammatory lesions, can also demonstrate increased uptake (5,6).

Imaging the DNA synthetic pathway is an alternative approach to imaging tumors because it may be more specific and better reflect treatment response. Thymidine labeled with ^{11}C was the initial tracer used and has shown promise in limited trials (7,8). The practical limitations of using ^{11}C -thymidine include its rapid biodegradation and the short half-life of ^{11}C , prompting researchers to look for other potential pyrimidine analogs, including 1-(2'-deoxy-2'-fluoro- β -D-arabinofuranosyl)thymine (FMAU), which can be labeled with either ^{11}C or ^{18}F (9-11). Previous studies have demonstrated that FMAU resists degradation and is incorporated into DNA but not into RNA or protein.

Our current study focused on imaging DNA synthesis using ^{18}F -FMAU, an antiviral and antineoplastic agent that has been administered to patients with advanced cancer (12,13). FMAU can be phosphorylated by thymidine kinase 1 and thymidine kinase 2 followed by DNA incorporation through DNA polymerase (14,15). In vitro studies have demonstrated that the level of FMAU incorporated into DNA is proportional to the level of DNA synthesis and the rate of proliferation. Furthermore, cell growth inhibition is proportional to the level of FMAU incorporated into DNA (16), suggesting that retention of FMAU within tumor cells should be a direct indicator of DNA synthesis and tumor proliferation when compared with other existing PET tracers. Our hypothesis stated that tumors and normal proliferating tissues such as bone marrow (with increased expres-

Received Feb. 12, 2004; revision accepted Sep. 15, 2004.
For correspondence or reprints contact: Anthony F. Shields, MD, PhD, Karmanos Cancer Institute, 4HWCR, 4100 John R St., Detroit, MI 48201.
E-mail: shieldsA@karmanos.org

sion of thymidine kinase 1 and DNA polymerase) will have increased uptake and retention of FMAU and thus show increased activity of ^{18}F -FMAU on PET images. Here, we report the first (to our knowledge) imaging studies of ^{18}F -labeled FMAU.

MATERIALS AND METHODS

We studied 5 normal dogs with body weights ranging from 14.2 to 18.6 kg. Two of the dogs had tissue samples obtained for analysis at 60 min after ^{18}F -FMAU injection without PET, whereas the other 3 were initially imaged with PET followed by tissue removal and analysis. The dogs were anesthetized with 5 mg of pentobarbital per kilogram of body weight per hour during the imaging study. The animal-subjects protocol for this study was reviewed and approved by the Committee on Animal Studies of Wayne State University.

PET Image Acquisition

We synthesized the ^{18}F -FMAU with a purity greater than 98% and specific activity greater than 111 GBq/ μmol as previously described (10) and intravenously injected into the dogs a dose ranging from 67 to 264 MBq over 60 s. A Harvard syringe pump was used to administer ^{18}F -FMAU in the PET study. Injection was manual for the 2 dogs used in the biodistribution studies without imaging.

Three dogs were imaged for up to 2.5 h, followed by tissue removal and analysis. Before tracer injection, a 15-min transmission scan was acquired to correct for photon attenuation. Dynamic PET was performed for 60 min using an Exact/HR tomograph (Siemens) with the field of view over the lower chest and upper abdomen, yielding a series of timed images of progressively longer duration (4×20 s, 4×40 s, 4×60 s, 4×180 s, and 8×300 s). The dynamic image sequence was reconstructed using a filtered backprojection algorithm applying a Hanning filter with a smoothing kernel of 13 mm in full width at half maximum.

After the dynamic acquisition, we acquired 1 whole-body PET scan. The whole-body scans included 6–7 bed positions (4 min of transmission and 6 min of emission per bed position) and were started about 65 min after injection. The whole-body images were reconstructed using an iterative ordered-subsets expectation maximization algorithm (2 iterations and 8 subsets) followed by a smoothing kernel of 13 mm in full width at half maximum. Blood samples were obtained from an intravenous catheter, different from the one used for tracer injection, at serial times (1, 2, 3, 4, 5, 6, 7, 9, 11, 15, 20, 30, 40, 50, 60, 90, 120, and 150 min) and were counted for total radioactivity by a NaI well counter (Cobra II; Packard), and a limited number of samples (5, 11, 15, 30, 60, and 150 min) were analyzed by high-performance liquid chromatography (HPLC) for metabolites. The urine samples obtained at 60 min and approximately 150 min after injection were counted for total radioactivity and analyzed by HPLC for metabolites. For the metabolite analysis, an ODS C-18 analytic column (250×4.6 mm; Hypersil) with a mobile phase of 10 mmol of NaOAc per liter in 6% acetonitrile was used. Twenty-five fractions at a 1 mL/min flow rate were collected. Meanwhile, all blood and urine samples were counted for total radioactivity.

Biodistribution Studies

The 3 dogs that underwent initial PET were sacrificed after imaging at times ranging from 151 to 162 min after injection. The

2 dogs that were not scanned were sacrificed at 60 min after injection using an overdose of pentobarbital. Tissue samples of selected organs were immediately removed, counted, and weighed to obtain the ^{18}F activity level in these organs. ^{18}F -FMAU retention in the tissue samples was quantified using the standardized uptake value (SUV), defined as the radioactivity per gram of tissue divided by the total injected radioactivity per gram of body weight. In addition, the selected tissue samples were homogenized, followed by the addition of 1 mL of perchloric acid (PCA) into each tube to precipitate the macromolecules containing DNA, RNA, and proteins and other macromolecules. To complete the extraction, we centrifuged the mixture at 15,000g at 4°C for 10 min to separate the pellet from the supernatant, followed by washing of the pellet 3 times with 1 mL of PCA (1 mol/L) and centrifugation. After extraction, the amount of radioactivity in the acid-soluble fraction and pellet that contained macromolecules including DNA was quantified, and the percentage of each corresponding fraction was calculated (17). Furthermore, the supernatants of 12 different tissue extracts and gallbladder fluids were analyzed using HPLC to determine the metabolite levels in these organs.

Image Data Analysis

Both the dynamic image sequence and the whole-body scan were decay corrected to the start times of the scan. Summed images from 30 to 60 min over all dynamic frames were used to define regions of interest (ROIs). ROIs were defined at the location of the normal tissues, such as heart, marrow, small intestine, and muscle. ROIs were defined with at least a 2-cm diameter to minimize the partial-volume effects. However, distortions due to partial-volume effect might have been present, especially in small anatomic structures such as the marrow. Regional tracer uptake values were quantified using SUV. Time-activity curves were obtained for all defined ROIs from the dynamic sequence. Regional time-activity curves were continued beyond 60 min by combining the initial data from the dynamic scan with the data from the whole-body scans. For each ROI, the time at which the corresponding organ was in the field of view was determined, and the activity was decay corrected to the start time of the dynamic image sequence. This step provided 1 additional point for each ROI beyond the time of the dynamic sequence.

RESULTS

In these normal dogs, ^{18}F -FMAU was selectively incorporated into the DNA of normal proliferating tissues and resisted degradation.

Accumulation of FMAU in the bone marrow was consistent with its retention in proliferating tissues (Fig. 1). FMAU was also found in the lymph nodes, small intestine, and stomach because of a certain degree of proliferation in these tissues. Furthermore, increased ^{18}F -FMAU activity could be visualized in the heart because of high levels of thymidine kinase 2. In addition, the kidneys could clearly be distinguished from background activity because of excretion (Fig. 1). ^{18}F -FMAU time-activity curves obtained from dynamic scans (Fig. 2) showed that ^{18}F -FMAU retention was significantly higher in the marrow than in the blood during the 2.5 h of the study. Furthermore, retention of radioactivity by bone marrow increased with time, whereas radioactivity in the blood and background decreased. Tracer



FIGURE 1. Attenuation-corrected projection (A) and sagittal (B) PET images of a dog 68–150 min after injection of 81.4 MBq of ^{18}F -FMAU show accumulation of ^{18}F -FMAU and increased activity in lymph nodes, small intestine, stomach, and marrow because of varying degrees of increased cell proliferation. Increased activity was also seen in heart because of high level of thymidine kinase 2.

concentration in the marrow was underestimated because of the limitation from partial volume. The time–activity curves were generated from the combination of dynamic scans and 1 whole-body scan of 2-dimensional images, which were reconstructed with different reconstruction algorithms. Although the different reconstruction algorithms may have led to different noise characteristics, it was valid to use an additional time point from the whole-body scan to extend the time–activity curve generated by dynamic scans, because the value pattern and the absolute values obtained from both types of scans were the same.

Imaging data were corroborated by obtaining tissue samples for analysis at the end of whole-body scanning. The results obtained from necropsy tissue analysis showed that the marrow-to-blood ratio was highest, at an average value of 12.3, followed by the ratio of small intestine to blood, at an average value of 7.0 (Table 1). These results demonstrated that FMAU accumulated readily in proliferating tissues such as bone marrow and were consistent with tracking of DNA synthesis by FMAU. In addition, the necropsy tissue analysis indicated that marrow had the highest SUV (3.9) at 160 min after injection, followed by small intestine, heart, stomach, lymph nodes, and kidneys, which had mean SUVs of 2.26, 1.78, 1.62, 1.44, and 1.28, respectively (Table 1). Furthermore, Table 1 demonstrates that FMAU retention increased with time in proliferating tissue such as marrow (e.g., SUVs of 1.1 at 60 min and 3.9 at 160 min) but decreased with time in nonproliferating tissues such as heart and kidneys (heart SUV of 2.68 at 60 min and 1.78 at 160 min; kidney SUV of 2.37 at 60 min and 1.28 at 160 min). ^{18}F -FMAU was distributed with tissue-to-muscle ratios of approximately 1.0 in nonproliferative organs such as lung, liver, and kidneys. Despite the fact that FMAU retention increased not only in proliferating tissue but also in some nonproliferating tissues, the tissue extract analysis demonstrated that 87.4% of the radioactivity in marrow and 64.4% of the radioactivity in small intestine was acid precipitable. Although these acid-precipitable

macromolecules could include DNA, RNA, proteins, and other macromolecules, previous studies reported that FMAU incorporates into DNA but not into either RNA or proteins (16). Therefore, we consider this acid-precipitable ^{18}F -FMAU consistent with incorporation into DNA. In contrast, more than 90% of the activity in nonproliferating tissues such as heart, lung, stomach, and kidneys was in the supernatant (Fig. 3). In addition, about 50% of the radioactivity in the lymph nodes was in the precipitate. Finally, HPLC analysis of blood and urine at 60 min after injection indicated that more than 95% of activity was present as intact ^{18}F -FMAU in blood and urine.

DISCUSSION

Previous studies demonstrated that FMAU could be incorporated into DNA and showed potential to be a proliferation marker for PET. We imaged 3 normal dogs with ^{18}F -FMAU and PET to investigate whether this tracer can be used to image DNA synthesis in proliferating tissues and if it can be developed as a clinical imaging agent. Our results (Table 1 and Fig. 3) demonstrated that 87.4% of the radioactivity in marrow, 64.4% of the radioactivity in small intestine, and 50% of the activity in lymph nodes was incorporated into DNA. Although the percentage of activity remaining in small molecules varied in these proliferative tissues, the absolute amounts, as measured by SUV, varied between only 0.5 and 0.8. By contrast, more than 90% of the

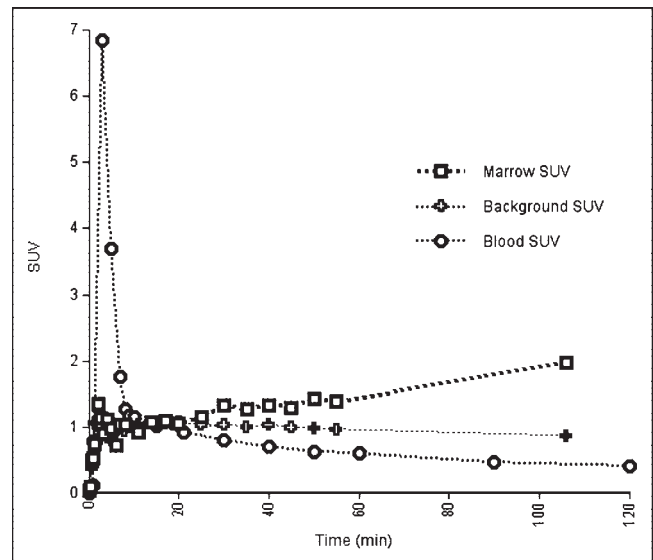


FIGURE 2. ^{18}F -FMAU retention curves for marrow, muscle, and blood of normal dog. Curves were obtained from dynamic PET with field of view over upper abdomen and lower chest, yielding a series of timed images for up to 60 min. Additional time point beyond 60 min was obtained from whole-body scan acquired about 65 min after injection. Estimate of time, 117 min after injection in this figure, was based on time when organ of interest was in field of view. Marrow activity was not corrected for partial volumes, and marrow-to-blood ratio was 12.3 in tissue samples removed at 160 min after injection.

TABLE 1
Summary of SUV and Tissue-to-Blood Ratio Obtained from Necropsy Tissue Analysis

Tissue	SUV (60 min after injection)		SUV (160 min after injection)	
	Mean SUV of 2 dogs	Mean tissue-to-blood ratio of 2 dogs	Mean SUV of 3 dogs	Mean tissue-to-blood ratio of 3 dogs
Marrow	1.10 (0.98–1.22)	2.56 (2.48–2.65)	3.90 (3.62–4.18)	12.30 (10.10–14.49)
Small intestine	2.19 (1.93–2.45)	5.28 (3.93–6.62)	2.26 (2.11–2.40)	7.00 (6.69–7.31)
Lymph nodes	1.86 (1.78–1.94)	4.43 (3.62–5.24)	1.44 (1.34–1.54)	4.49 (4.30–4.67)
Stomach	1.79 (1.75–1.82)	4.22 (3.70–4.73)	1.62 (1.60–1.63)	5.05 (4.54–5.55)
Heart	2.68 (2.34–3.02)	6.45 (4.75–8.16)	1.78 (1.66–1.89)	5.50 (5.28–5.73)
Kidneys	2.37 (2.20–2.54)	5.67 (4.48–6.86)	1.28 (1.20–1.35)	4.00 (3.33–4.67)
Liver	2.01 (1.70–2.32)	4.87 (3.46–6.27)	0.92 (0.80–1.03)	2.90 (2.23–3.56)
Spleen	1.50 (1.24–1.76)	3.46 (3.35–3.57)	1.07 (1.06–1.08)	3.34 (2.95–3.73)
Lung	1.15 (0.92–1.38)	2.80 (1.86–3.73)	0.93 (0.92–0.95)	2.92 (2.64–3.19)
Muscle	0.65 (0.50–0.80)	1.59 (1.02–2.16)	0.98 (0.96–1.01)	3.06 (2.77–3.34)
Blood	0.43 (0.37–0.49)	1.00 (1.00–1.00)	0.32 (0.29–0.36)	1.00 (1.00–1.00)
Gallbladder	0.79 (0.02–1.56)	1.61 (0.05–3.18)	6.84 (5.78–7.89)	22.26 (20.04–24.48)

n = 5. Data in parentheses are ranges.

radioactivity in the nonproliferating tissues, such as heart and kidneys, was in the supernatant, although increased activity could be seen both on the PET images and in tissues removed at autopsy. In addition, retention of FMAU in proliferating tissues increased with time, whereas retention of FMAU in nonproliferating tissues decreased with time. Further studies are needed to determine whether the level of FMAU incorporation is proportional to the rate of proliferation increase. In view of the evidence that FMAU has the same metabolic pathway as thymidine (18), we conclude that FMAU is a direct proliferation marker and that the use of ^{18}F -FMAU for in vivo imaging of DNA synthesis is feasible.

For decades, investigators have been seeking relatively ideal tracers to image tumor and DNA synthesis with PET. Thymidine has been labeled with ^{11}C for imaging tumor proliferation with PET and, because it can rapidly be incorporated into newly synthesized DNA, has been shown to be

better than ^{18}F -FDG as a marker for detecting tumor response after successful therapy (8). Unfortunately, its rapid in vivo degradation and the short half-life of ^{11}C (20 min) has impaired both the imaging quality and the calculation of proliferation rates with thymidine. ^{18}F -Labeled 3'-deoxy-3'-fluorothymidine (FLT) is being tested since it is resistant to degradation and accumulates favorably in several types of human cancer (19,20). However, FLT is not a direct marker for DNA synthesis because most FLT cannot be incorporated into DNA. Therefore, FLT measures only cellular thymidine kinase activity, although phosphorylation and thus trapping of FLT correlate with DNA synthesis (21). In contrast, FMAU can be taken up by the cells and then phosphorylated by thymidine kinase 1, followed by DNA incorporation through DNA polymerase (18). Therefore, imaging with ^{18}F -FMAU may provide data complementary to those provided by FLT, which is trapped in the cell as FLT phosphate by thymidine kinase alone. Furthermore, consistent with previous studies (11), HPLC analysis of blood and urine samples obtained at 60 min after injection demonstrated that more than 95% of the activity was present as intact FMAU, indicating that FMAU resists degradation in vivo.

CONCLUSION

Further clinical studies are needed to evaluate FMAU imaging of tumors. Limitations imposed by uptake of FMAU in normal heart, kidneys, and liver also need to be determined. Finally, it would be worthwhile to compare ^{18}F -FMAU with ^{18}F -FLT and other proliferation markers to determine their retention and clinical application. In summary, we produced ^{18}F -FMAU with high purity and performed in vivo imaging of DNA synthesis with ^{18}F -FMAU and PET. The ability to image and measure DNA synthesis in vivo can provide an important tool for clinical applica-

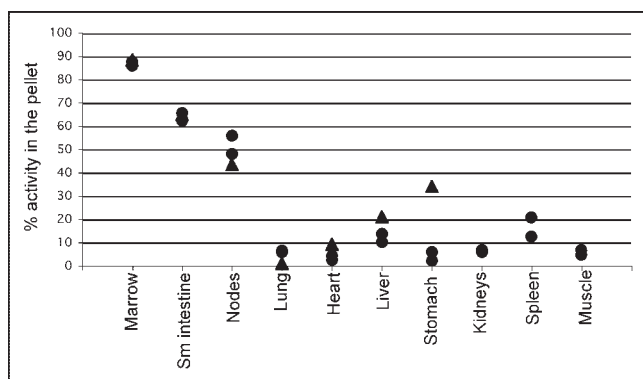


FIGURE 3. FMAU DNA incorporation (*n* = 3). Three normal dogs were used for this study. One dog was sacrificed at 160 min after injection (▲), and the other 2 dogs were sacrificed at 60 min after injection (●). All tissue samples were analyzed by acid precipitation to determine DNA fraction. Sm = small.

tions in the diagnosis of tumors and in surveillance of tumor development and impact of antitumor therapy.

ACKNOWLEDGMENTS

The authors thank Dr. Elizabeth Dawe for veterinary assistance and Theresa A. Jones for expert technical assistance with the PET studies. This work was partially supported by funding from the National Cancer Institute, grants CA 83131 and CA 82645.

REFERENCES

1. Krohn KA. Evaluation of alternative approaches for imaging cellular growth. *Q J Nucl Med.* 2001;45:174–178.
2. Kostakoglu L, Coleman M, Leonard JP, Kuji I, Zoe H, Goldsmith SJ. PET predicts prognosis after 1 cycle of chemotherapy in aggressive lymphoma and Hodgkin's disease. *J Nucl Med.* 2002;43:1018–1027.
3. Romer W, Hanauske A, Ziegler S, et al. Positron emission tomography in non-Hodgkin's lymphoma: assessment of chemotherapy with fluorodeoxyglucose. *Blood.* 1998;91:4464–4471.
4. Shields A. Monitoring treatment response. In: Wahl R, ed. *Principles and Practice of Positron Emission Tomography.* Philadelphia, PA: Lippincott; 2002: 252–267.
5. Yamada Y, Uchida Y, Tatsumi K, et al. Fluorine-18-fluorodeoxyglucose and carbon-11-methionine evaluation of lymphadenopathy in sarcoidosis. *J Nucl Med.* 1998;39:1160–1166.
6. Kubota R, Yamada S, Kubota K, Ishiwata K, Tamahashi N, Ido T. Intratumoral distribution of ¹⁸F-fluorodeoxyglucose in vivo: high accumulation in macrophages and granulation tissues studied by microautoradiography. *J Nucl Med.* 1992;33:1972–1980.
7. Eary JF, Mankoff DA, Spence AM, et al. 2-[C-11]thymidine imaging of malignant brain tumors. *Cancer Res.* 1999;59:615–621.
8. Shields AF, Mankoff DA, Link JM, et al. [¹¹C]Thymidine and FDG to measure therapy response. *J Nucl Med.* 1998;39:1757–1762.
9. Wang H, Oliver P, Nan L, et al. Radiolabeled 2'-fluorodeoxyuracil-beta-D-arabinofuranoside (FAU) and 2'-fluoro-5-methyldeoxyuracil-beta-D-arabinofuranoside (FMAU) as tumor-imaging agents in mice. *Cancer Chemother Pharmacol.* 2002;49:419–424.
10. Mangner T, Klecker R, Anderson L, Shields A. Synthesis of 2'-[¹⁸F]fluoro-2'-deoxy-β-D-arabinofuranosyl nucleotides, [¹⁸F]FAU, [¹⁸F]FMAU, [¹⁸F]FBAU and [¹⁸F]FIAU, as potential PET agents for imaging cellular proliferation. *Nucl Med Biol.* 2003;215–224.
11. Conti P, Alauddin M, Fissekis J, Schmall B, Watanabe K. Synthesis of 2'-fluoro-5-[¹¹C]-methyl-1-beta-D-arabinofuranosyluracil ([¹¹C]-FMAU): a potential nucleoside analog for in vivo study of cellular proliferation with PET. *Nucl Med Biol.* 1995;22:783–789.
12. Fanucchi MP, Leyland-Jones B, Young CW, Burchenal JH, Watanabe KA, Fox JJ. Phase I trial of 1-(2'-deoxy-2'-fluoro-1-beta-D-arabinofuranosyl)-5-methyluracil (FMAU). *Cancer Treat Rep.* 1985;69:55–59.
13. Abbruzzese JL, Schmidt S, Raber MN, et al. Phase I trial of 1-(2'-deoxy-2'-fluoro-1-beta-D-arabinofuranosyl)-5-methyluracil (FMAU) terminated by severe neurologic toxicity. *Invest New Drugs.* 1989;7:195–201.
14. Lewis W, Levine ES, Griniuviene B, et al. Fialuridine and its metabolites inhibit DNA polymerase gamma at sites of multiple adjacent analog incorporation, decrease mtDNA abundance, and cause mitochondrial structural defects in cultured hepatoblasts. *Proc Natl Acad Sci USA.* 1996;93:3592–3597.
15. Lu L, Samuelsson L, Bergstrom M, Sato K, Fasth KJ, Langstrom B. Rat studies comparing ¹¹C-FMAU, ¹⁸F-FLT, and ⁷⁶Br-BFU as proliferation markers. *J Nucl Med.* 2002;43:1688–1698.
16. Collins JM, Klecker RW, Katki AG. Suicide prodrugs activated by thymidylate synthase: rationale for treatment and noninvasive imaging of tumors with deoxyuridine analogues. *Clin Cancer Res.* 1999;5:1976–1981.
17. Shields AF, Lim K, Grierson J, Link J, Krohn KA. Utilization of labeled thymidine in DNA synthesis: studies for PET. *J Nucl Med.* 1990;31:337–342.
18. Bading JR, Shahinian AH, Bathija P, Conti PS. Pharmacokinetics of the thymidine analog 2'-fluoro-5-[(14C)-methyl-1-beta-D-arabinofuranosyluracil] ([¹⁴C]FMAU) in rat prostate tumor cells. *Nucl Med Biol.* 2000;27:361–368.
19. Shields AF. Labeled pyrimidines in PET imaging. In: Valk PE, Bailey DL, Townsend DW, Maisey MN, eds. *Positron Emission Tomography.* London, U.K.: Springer-Verlag; 2003:715–724.
20. Shields A, Grierson J, Dohmen B, et al. Imaging proliferation in vivo with [¹⁸F]FLT and positron emission tomography. *Nat Med.* 1998;4:1334–1336.
21. Sherley JL, Kelly TJ. Regulation of human thymidine kinase during the cell cycle. *J Biol Chem.* 1988;263:8350–8358.